Non-Rapid Eye Movement Sleep Features in Post-Stroke Human Electroencephalogram

Benjamin K. Simpson[1, *], Rohit Rangwani[2,3, *], Aamir Abbasi[2],
Jeffrey M. Chung[1], Chrystal M. Reed[1, #], Tanuj Gulati[1,2,3,4, #]

[1] Department of Neurology, Cedars-Sinai Medical Center, Los Angeles, CA.
[2] Center for Neural Science and Medicine, Department of Biomedical Sciences, Cedars-Sinai Medical Center, Los Angeles, CA.
[3] Bioengineering Graduate Program, Department of Bioengineering, Henry Samueli School of Engineering, University of California - Los Angeles, Los Angeles, CA.
[4] Department of Medicine, David Geffen School of Medicine, University of California-Los Angeles, Los Angeles, CA.

* These authors contributed equally
[#] These authors contributed equally

Correspondence: tanuj.gulati@csmc.edu

Abstract

Background

Sleep is known to promote recovery post-stroke. However, there is a paucity of data profiling nested sleep oscillations post-stroke in the human brain. Recent rodent work showed that resurgence of physiologic spindles coupled ('nested') to sleep slow oscillations (SOs) and concomitant decrease in pathological delta (δ) waves is associated with sustained motor performance gains during stroke recovery. This work also showed that post-injury sleep could be pushed toward a physiological state via a pharmacological reduction of tonic γ-aminobutyric acid (GABA). The goal of this project is to evaluate non-rapid eye movement (NREM) sleep oscillations (namely, SOs, spindles and δ waves, and their nesting) in the post-stroke human brain.

Methods

We analyzed NREM-marked electroencephalography (EEG) data in human stroke patients who were hospitalized for stroke and received EEG monitoring as part of their clinical workup. Electrodes were classified as 'stroke' (immediate peri-infarct areas) or 'contralateral' (unaffected hemisphere). We used linear mixed-effect models to investigate effects of stroke, patients and concurrent pharmacologic drugs they were on during EEG data capture.

Results

We found significant fixed and random effects of stroke, patients, and pharmacologic drugs on on different NREM sleep oscillations. Most patients showed increase in δ waves in *stroke* versus *contralateral* electrodes. However, for patients on propofol and scheduled dexamethasone, δ wave density was high in both hemispheres. SO density followed the same

trend seen in δ wave density. δ wave-nested spindles, that are considered harmful to recovery related plasticity, were high in groups who received propofol or levetiracetam.

Conclusions

These findings suggest that, acutely post-stroke, pathological δ waves increase in the human brain and that spindle density may be impacted by drugs that modulate excitatory/inhibitory neural transmission. Further, we found that drugs that increase inhibitory transmission or curb excitation promote pathological δ wave-nested spindles. Our results indicate that factoring in pharmacologic drugs may be important when targeting sleep modulation for neurorehabilitation.

Keywords: Stroke, Sleep, EEG

Introduction

Stroke is a leading cause of motor disability world-wide, and despite advances in rehabilitation, there is a lack of widely adopted therapies that target plasticity and functional outcomes remain inconsistent [1–3]. Sleep is known to play a major role in regulating plasticity [4–12] and accordingly, there has been an interest in modulating sleep for stroke motor rehabilitation[13,14]. To optimize efforts to modulate sleep effectively, there is a need to better understand neural processing during sleep, as well as the effect of practical scenarios including patient co-morbidities and concurrent pharmaceuticals that may impact excitatory/inhibitory neural transmission. While a whole host of studies in animals and humans have shown that sleep can influence motor recovery post-stroke[2,14–23], more work is needed to understand how sleep neurophysiology is affected in stroke, as well as inter-individual variations in human stroke patients. This has become all the more important with advances in our understanding of sleep neurophysiology linking nested non-rapid eye movement (NREM) oscillations to plasticity, motor memory consolidation, and motor recovery[4,6,14,24].

Sleep-dependent neural processing is crucial for memory consolidation – the process of transferring newly learned information to stable long-term memory[9,25]. While this process is well-studied for hippocampal-dependent declarative memory systems[26–28]; seminal advancements have now been made to understand how sleep benefits motor learning[5,6,24,29,30]. Specifically, NREM sleep has been linked to reactivation of neural ensembles associated with movement control and performance gains in a motor skill after sleep[4–6]. Of note, there is increasing consensus that this consolidation occurs during precise temporal coupling of sleep spindles (10–16 Hz) to larger amplitude slow oscillations (SOs, 0.1–1Hz)[6,25,31–35]. Recent work in rodents has shown that these SOs nested with spindles decline immediately post-stroke and track motor recovery on a dexterous reach-to-grasp motor task[14]. This work also showed that delta waves (δ

waves, 1–4Hz) increased immediately post-stroke and reduced, along with *δ* waves nested with spindles, during recovery. Our chief goal was to see if NREM oscillations and their nesting were similarly affected post-stroke in human patients within a hospital setting, one within the framework of real-world stroke management including co-morbidities and dissimilar pharmaceuticals that may modulate neural transmission.

Recent work has laid out important principles regarding how NREM sleep features are linked to learning of a novel motor skill in an intact brain, and it has become imperative to profile these sleep features in a stroke brain. Work has shown that the balance between global SOs and the local slow-waves, i.e., *δ* waves determines whether there is an enhancement ('strengthening') or detraction ('forgetting') of motor skill[6]. This principle was extended to a rodent stroke model where an investigation of sleep microarchitecture, acutely post-stroke, revealed that *δ* waves predominated the cortex relative to SOs (thereby impairing sleep-associated 'strengthening' of memory or recovery-related reorganization) and that this balance was flipped as spontaneous recovery occurred and sleep neural processing was rescued from the 'forget' state[14]. Importantly, this work also showed that pharmacological reduction of tonic γ-aminobutyric acid (GABA) neurotransmission accelerated sleep's natural neural processing that serves a motor memory 'strengthening' purpose. The prevalence of local low-frequency power (< 4Hz) during spontaneous periods has also been reported in previous studies of human stroke patients[22,36–38] and in animal stroke models[39–42], but the nesting of spindles to SOs versus *δ* waves is an important recent advance in rodent research without human correlation. We wanted to profile this NREM activity in human stroke patients acutely post-stroke as the nesting of spindles to slow waves may have a role in setting brain states amenable to motor memory strengthening versus forgetting.

Our study showed that, acutely post stroke, there is an increase in SOs and δ waves on stroke electrodes when compared to contralateral hemisphere electrodes, and our linear mixed effect model revealed that there was a significant random effect of concurrent pharmacologic drug (propofol, dexamethasone, levetiracetam). The patient that received propofol and dexamethasone had increased slow-waves in both hemispheres, and the patient that received levetiracetam had a significantly higher number of spindles on stroke electrodes. In all patients (grouped by being on propofol and dexamethasone or levetiracetam or other drugs that do not interact with GABAergic/glutamatergic transmission the brain), we saw that density of δ waves-nested spindles was higher than SO-nested spindle and that this density was highest in the patient who received propofol and dexamethasone, followed by levetiracetam group, and then the “other drug” group. We observed similar trends for SO-nested spindles, but overall, densities were lower compared to δ wave nested spindles. Together, our work suggests that acute stroke care management should incorporate pharmacologic drug interactions and their effect on ‘restorative’ sleep oscillations. This may help inform a personalized approach to sleep modulation for neurorehabilitation.

Methods

Ethics, consent and permissions

This research was conducted in accordance with and approval of the Cedars-Sinai Medical Center Institutional Review Board (IRB). All research participants and/or their surrogates provided informed consent to participate in the study. This study adhered to Strengthening the Reporting of Observational Studies in Epidemiology (STROBE) guidelines for cohort studies[43].

Inclusion/exclusion criteria

Retrospective chart review of the Cedars-Sinai EEG database was done to identify patients with acute, large vessel strokes who also received EEG monitoring as part of their hospital stay. Five patients were chosen for this study, with notably limited availability of EEG studies done within 2-3 days after an MCA (middle cerebral artery) distribution stroke. All patients were seen acutely for stroke at Cedars-Sinai and received EEG monitoring post-stroke. All patients were monitored between 2016 and 2021. Data was collected and analyzed between 2020 and 2023. Relevant clinical data was obtained from the Cedars-Sinai electronic medical record. Of the 5 patients, 3 were female and 2 male, all within the age range of 50–70 years old. Indications for EEG were universally for altered mental status after acute stroke. P2 (Patient 2) was noted to have partial status epilepticus involving the right temporal lobe (also see **Table 1** for tabulated clinical information on all patients). No seizures were reported in the any other patients' recordings. A total of ~5.9801 ± 1.2563 hours (or 358.8036 ± 75.4 mins) of NREM sleep was analyzed in the five patients.

Subjects were excluded if they met any of the following criteria: currently pregnant or with a history of craniotomy. Our dataset is confined to five patients here as it is relatively rare to have stroke patients receive epilepsy monitoring, and due to further eligibility criteria that we had set (such as an MCA stroke; also see the Discussion section on limitations).

EEG analysis and identification of NREM oscillations

Patients with overnight EEG studies 2 to 3 days post-stroke, with appropriate clinic follow up, were included. The data, obtained by a Natus Xltek EEG and Sleep System, was de-identified and made compatible for analysis with MATLAB. Each 30-second epoch was individually and manually marked by an expert scorer (C.M.R. and B.K.S.) for NREM sleep. EEG epochs were analyzed for identifying NREM sleep in a bipolar montage. The following analysis was done with EEG data in a referential montage, referenced to the auricle electrodes. Spindles, SOs, and *δ* waves were extracted from these NREM epochs using custom code in MATLAB (details below). This allowed for the identification of specific sleep waveforms and how they nested temporally and topographically during NREM sleep. An emphasis was placed on assessing spindles and their nesting to SOs and *δ* waves. Topographical maps of the average density of these sleep waveforms allowed us to visualize the average densities with respect to electrode location.

EEG Data processing:

NREM-marked EEG data from all channels was referenced with respect to the average of the auricular electrodes (A1 & A2, **Fig. 1**). Any high amplitude artifact in the differential EEG signal was removed. This data was filtered into the frequency ranges of 0.1-4 Hz for *δ*/SOs identification and 10-16 Hz for spindle detection. For ***δ/SOs detection***, signal was first passed through a 0.1 Hz high-pass filter and then a 4 Hz low-pass Butterworth filter. All positive-to-negative zero crossings, previous peaks, following troughs, and negative-to-positive zero crossings were identified. A wave was considered a *δ* wave if its trough was lower than the negative threshold and preceded by a peak that was lower than the positive threshold, within 500 ms (**Fig. 2A, B**). SOs were classified as waves with troughs lower than a negative threshold

(the bottom 40 percentile of the troughs) and preceding peaks higher than a positive threshold (the top 15 percentile of the peaks), shown in **Fig. 2C, D**. Duration between peaks and troughs was between 150 ms and 500 ms. For ***spindle detection***, EEG data was filtered using a 10 Hz high-pass Butterworth filter and a 16 Hz low-pass Butterworth filter. A smoothed envelope of this signal was calculated using the magnitude of the Hilbert transforms with convolving by a Gaussian window (200 ms). Epochs with signal amplitude higher than the upper threshold (mean, $\mu + 2.5*s.d., \sigma$) for at least one sample and amplitude higher than the lower threshold ($\mu + 1.5*\sigma$) for at least 500 ms were considered spindles (**Fig. 2E, F**). The lower threshold was used to define the duration of the spindle. Nested SO-spindles (similar to *k*-complexes studied in humans) were identified as spindle peaks following SO peaks within 1.5 s duration (**Fig. 2G**). The same criterion was used to identify δ wave-nested spindles as shown in **Fig. 2H**.

<u>Data Analysis:</u>

We generated topographical maps of these different waveforms using *plot_topography* function in MATLAB[44] as shown in **Fig. 3**. The patients were separated into 3 different groups based on concurrent medications as shown in **Table 1**. Patient 1 was assigned to Group 1, who was on continuous propofol and dexamethasone injections every four hours. Group 2, patients 2 and 5, was administered levetiracetam (Keppra) twice daily, and Group 3, comprised of patients 3 and 4, was not on any medications known to significantly modulate excitatory/inhibitory neural transmission.

Perilesional electrodes were identified by analyzing post-stroke MRI and CT brain imaging. We marked ‘Stroke electrodes’ as the electrodes covering the perilesional region of the brain as shown in **Fig. 1**. The mirror opposite electrodes on contralateral side were marked as “Contralateral electrodes’ for further analysis.

Statistical Analysis

We performed a linear mixed effect analysis for all patients comparing the *Stroke electrodes* density vs Co*ntralateral electrodes* density for different waveforms using the *fitlmematrix* function in MATLAB.

The linear mixed effect model was fitted by maximum likelihood using the formula below **(1)** for all the different waveforms identified during EEG data processing. Medication groups were defined as the 3 groups as mentioned earlier. This model considers fixed effects of stroke vs contralateral electrodes, and the random effect of electrodes and medication groups depending on the patient.

Waveform Density ~ 1 + Electrode + (1 + Electrode + Medication Groups | Patient) (1)

We also compared the *Stroke electrodes* density vs Co*ntralateral electrodes* density within each medication group using a two-tailed *t*-test. One-way ANOVA was used to compare the stroke electrodes' NREM oscillations' density of the 3 different medication groups.

We calculated r-squared, and the Cohen's *d* values from the linear mixed effect model. Cohen's *d* was used to evaluate if the nested data for NREM oscillations in different medication groups had a small, medium or large experimental effect (Cohen's d = 0.20, 0.50 or 0.80, respectively)[45].

Results

One of the limitations of retrospectively analyzing EEG data gathered from clinical EEG was the heterogeneity encountered across the subjects studied, a contrast from the controlled setting of related rodent studies. Knowing this, we found that one important similarity across the study population was the indication for EEG: concern for underlying seizure in the setting of altered mental status and recent hemispheric stroke. Accordingly, the patients were all hospitalized, and our analysis benefited from close pharmacologic documentation. We identified concurrent medications to be a major confounding variable, particularly medications that influenced neural transmission. Trends were analyzed with attention to this variable. P1 was noted to be on continuous infusion of propofol and infusions of dexamethasone every 4 hours. P2 and P5 were treated with levetiracetam 500mg twice daily. P3 and P4 were not given propofol, dexamethasone, or levetiracetam.

SO and *δ* wave density increased in perilesional electrodes

Consistent with previous reports, we found that stroke electrodes had higher < 4 Hz oscillations (*δ*)[46]. Our mixed-effects model showed a significant fixed effect of stroke vs contralateral electrodes for a subset of NREM oscillations and a large effect of concurrent pharmaceuticals. Overall, we observed higher *δ* waves density in the perilesional electrodes (**Fig. 4B**; linear mixed-effects model: t_{42} = 3.6979, p = 0.0006, R^2 = 0.4317; Cohen's d = 0.9517). P1, the patient on continuous propofol and frequent dexamethasone, showed a trend of higher *δ* wave density in perilesional and contralateral electrodes. The propofol and dexamethasone group and the non-neuromodulatory drug group both had higher *δ* wave density on stroke electrodes than the levetiracetam group (**Fig. 4B**; Group 1: 11.2315 ± 2.5270 counts min^{-1} (mean ± s.e.m.); Group 2: 9.0653 ± 1.3206 counts min^{-1}; Group 3: 12.2454 ± 1.5866 counts min^{-1}; one-way ANOVA, $F(2,19) = 0.97$; $p = 0.3983$). Only the levetiracetam and non-neuromodulatory group

showed a significantly high density of δ waves in the perilesional electrodes vs contralateral electrodes. We observed similar trends for SOs, and there was a medium effect of the medication grouping along with a significant fixed effect of stroke vs contralateral electrodes (t_{42} = 3.0559, p = 0.0039, R^2 = 0.3316 and Cohen's d = 0.7029). The patients who received propofol and dexamethasone or levetiracetam did not show a significant difference between stroke or contralateral electrode SO density. However, the patients who did not receive neuromodulatory medications showed significantly more SO density on stroke electrodes, as shown in **Fig. 4C** (two-tailed t-test, t_{20} = 2.4167, p = 0.0253). Notably, SOs on stroke electrodes were highest in this group when compared to the patients that belonged to groups that received propofol and dexamethasone or levetiracetam (**Fig. 4C**; Group 1: 2.9134 ± 0.7147 counts min^{-1}; Group 2: 2.4204 ± 0.3701 counts min^{-1}; Group 3: 3.2858 ± 0.4464 counts min^{-1}; one-way ANOVA, $F(2,19)$ = 0.9; p = 0.4227).

Our linear mixed-effects model did not show a significant fixed effect of stroke versus contralateral electrodes on spindle density, however, overall, it was a large effect based on the Cohen's d (**Fig. 4D;** linear mixed-effects model; t_{42} = 0.8516, p = 0.3993, R^2 = 0.3969 and Cohen's d = 0.8649). Spindle density was the highest on the stroke electrodes in the patient receiving propofol and dexamethasone (8.0037 ± 0.8763 counts min^{-1}), followed by the patients receiving levetiracetam (6.8267± 0.7872 counts min^{-1}), and followed by patients not on neuromodulatory medications (5.6120 ± 0.4366 counts min^{-1}) (**Fig. 4D**, one-way ANOVA, $F(2,19)$ = 3.1; p = 0.0681). The levetiracetam group had significantly elevated spindle density on stroke electrodes versus contralateral electrodes (**Fig. 4D** (middle, group 2); stroke: 6.8267± 0.7872 counts min^{-1}; contralateral: 4.2715 ± 0.7526 counts min^{-1}; two-tailed t-test, t_{12} = 2.3462, p = 0.0370). Patients who did not receive the neuromodulatory drugs did not show a significant difference between spindle density on electrodes from either hemisphere (**Fig. 4D** (right, Group

3); stroke: 5.6120 ± 0.4366 counts min^{-1}; contralateral: 5.5264 ± 0.9593 counts min^{-1}; two-tailed *t*-test, t_{20} = 0.0812; p = 0.9361).

δ wave-nested and SO-nested spindles.

Along with analyzing isolated NREM oscillations, we also looked at nested spindle densities. Similar to the recent rodent literature, we found that δ wave-nested spindles were increased acutely post-stroke. While our linear mixed effects model on δ wave-nested spindles did not show a significant difference between stroke and contralateral electrodes(linear mixed-effects model: t_{42} = 0.5686, p = 0.5727, R^2 = 0.5058 and Cohen's d value = 1.1728), we did observe a striking elevation of δ wave-nested spindles on stroke electrodes in the patient on propofol and dexamethasone (**Fig. 4E** (left); 3.4911 ± 0.3032 counts min^{-1}). This elevation was followed by the δ wave-nested spindle density of the levetiracetam group (**Fig. 4E** (middle); 3.2476 ± 0.4770 counts min^{-1}), and this group also had significantly elevated δ wave-nested spindle density on stroke electrodes versus contralateral electrodes (**Fig. 4E** (middle); contralateral: 1.9020 ± 0.3799 counts min^{-1}; two-tailed *t*-test, t_{12} = 2.2067, p = 0.0476). Finally, patients in the group not on neuromodulatory drugs (group 3) had a non-significant but lower δ wave-nested spindle density on stroke electrodes. (**Fig. 4E,** stroke: 2.7031 ± 0.2032 counts min^{-1}; one way ANOVA**,** $F(2,19)$ = 1.47; p = 0.2546) .

SO-nested spindles, that are postulated to augment reparative motor plasticity, were fewer in all patients acutely post-stroke (linear mixed-effects model: t_{42} = 0.8245, p = 0.4143, R^2 = 0.43 and Cohen's d = 0.9524). We did not observe a significant difference between stroke and contralateral electrodes in any of the three groups. SO-nested spindle density was not remarkably different on stroke electrodes between the three groups (**Fig. 4F**; Group 1: 0.9150 ± 0.1111 counts min^{-1}; Group 2: 0.8583 ± 0.1751 counts min^{-1}; Group 3: 0.6828 ± 0.0576 counts

min^{-1}; one-way ANOVA $F(2,19) = 1.16$; $p = 0.3352$). Notably, SO-nested spindle density was lower than δ waves-nested spindle density in all three groups' stroke electrodes.

Together, these results show that δ waves-nested spindles, deemed pathological by recent rodent research, were elevated in patients who received propofol, dexamethasone, and levetiracetam.

Discussion

Our results show that, similar to recent rodent findings, human stroke patients have a preponderance of δ wave-nested spindles in NREM sleep acutely after a stroke. Furthermore, we found that this trend was exacerbated by drugs like propofol and levetiracetam. These results extend the recent rodent results on pathological sleep oscillations to human stroke patients. These findings suggest a roadmap for delineating pathological sleep and optimal therapeutic modulation to promote recovery.

Sleep and plasticity post-stroke

Preclinical and clinical studies that have evaluated local-field potentials (LFPs) in animals[39,40] and EEG in patients[22,36,37] have found increased low-frequency power during awake, spontaneous periods after a stroke. These studies postulate that this increased low-frequency activity could be a marker of cortical injury and loss of subcortical inputs[47]. Our findings on increased δ waves are indicative of similar phenomena. We also found an increase in δ wave-nested spindles, with growing evidence that temporal coupling of spindles to SOs is a primary driver of sleep-related plasticity and memory consolidation[6,32–35,48,49]. SO-nested spindles are linked to spike-time dependent plasticity[50]. These events are also related to reactivation of awake experiences[28,32,48]. Importantly, disruption of this coupling can impair sleep-related memory consolidation of awake experiences[6]. This same work showed that SO-nested spindles and δ wave-nested spindles compete to either strengthen or forget a memory. Our results show that δ wave-nested spindles increased acutely after stroke and more so on stroke electrodes than contralateral electrodes. These are related to impaired sleep-processing that such nested oscillations were enhanced further by drugs such as propofol and levetiracetam. Our observations are consistent with other observations where propofol resulted in reduced SO-

nested high frequency oscillations[51,52]. It may be important to consider avoiding drugs that push sleep towards a pathological state, acutely after a stroke[53–55].

Propofol and Levetiracetam: effect on sleep

Propofol is one of the most commonly used anesthetics in neurologic intensive care units after stroke or traumatic brain injury[56]. It exerts its action by potentiating the activity of chloride currents through GABA receptors while blocking voltage-gated sodium channels[57–59]. Levetiracetam is a relatively newer anti-seizure drug. The exact mechanism for its anti-seizure mechanism is unclear, but it is believed to exert its effect through synaptic vesicle glycoprotein 2A[60]. Through this mechanism, levetiracetam is capable of modulate excitatory / inhibitory neurotransmission by inhibiting calcium currents[61]. Some studies have shown that levetiracetam has minimal effect on sleep parameters like total sleep duration, sleep latency, and sleep efficiency in both healthy humans and partial epilepsy patients[62]. However, observations have been made that levetiracetam can reduce motor activity and cause drowsiness during the day in patients treated with it[62,63]. Propofol, by its GABAergic action, causes greater loss of faster frequencies during induction with a shift in alpha frequencies to the frontal regions that reverses post-awakening[64–66]. In our study, the two groups that received medications that potentiate inhibitory GABA (levetiracetam or propofol) showed an increase pathological δ wave-nested spindles. Our results with limited dataset here suggests that levetiracetam impacted restorative sleep oscillations to a lesser extent than propofol.

Sleep processing and stroke rehabilitation

Recent rodent work profiled SO-nested and δ wave-nested spindles during the course of stroke recovery and found links between these nested structures and motor performance gains during recovery[6]. This work specifically looked into gains on reach-training, but clinical rehabilitation approaches can be varied[67–69]. It is likely that the sleep features of nested oscillations and their

putative pathological or physiological roles need to be factored in when considering timing for rehabilitation, irrespective of training type. Previous human and rodent studies have also suggested critical periods in training can offer long-term benefits[70–72]. Past studies that have found awake low-frequency power in stroke patients might be related to our findings of increased δ waves and δ wave-nested spindles. Future studies where EEG data is captured over the long term may delineate a transition from δ wave predominant sleep (pathological) to SO-nested spindle predominant sleep (physiological), and its relation to critical periods post-stroke for optimal timing of rehabilitation.

Modulation of sleep as a therapeutic intervention

The results we have presented can form the basis of translational studies in the future that target modulation of sleep post-stroke. Animal studies have suggested that modulation of GABAergic transmission (specifically $GABA_A$-receptor mediated tonic inhibition) in the perilesional cortex can serve as a therapeutic target to promote recovery, and that blocking of $GABA_A$-mediated tonic inhibition promoted motor recovery, this effect maximal in the first 1 to 2 weeks post-stroke[73,74]. Both short-term (acute) and long-term chronic infusion of $GABA_A$ inhibiting compounds have been tested, and long-term infusion was shown to be better[73]. Long-term pharmacologic modulation as shown by Clarkson and colleagues may be essential to achieve observable motor benefits in human patients. Benefits of long-term infusion include the effect of the drug not only with rehabilitation-specific online (awake) training, but also during offline memory consolidation during sleep.

Studies such as ours can also help guide electrical stimulation-based neuromodulation for augmenting recovery. SOs and δ waves can be easily monitored using EEG in stroke patients and modulated. Non-invasive brain stimulation during sleep[32,48,75,76] can be optimized to

suppress δ waves or boost SOs. Invasive stimulation approaches such as epidural stimulation[77] can also focus on sleep state to optimize sleep neural processing. Similar approaches have shown that direct epidural, motor cortical electric stimulation can enhance awake performance and neural activity[78,79] and epidural stimulation of subcortical regions can also modulate low-frequency oscillations in the motor cortex[80], however such approaches have not been applied during sleep. A recent study suggested modulating up states during sleep can enhance recovery[18]. It is plausible that future approaches targeting sleep, when delivered in a closed-loop fashion optimizes both awake task performance and its consequent sleep processing, may lead to greater long-term benefits during rehabilitation. Such treatments will also need to factor in concurrent pharmacologic drugs to target optimal density of SOs versus δ waves for specific time periods of rehabilitation training and sleep.

Limitations

One of the limitations of our study is lack of a link between sleep architecture and motor status. Future work that studies sleep over several days post-stroke and assesses motor functionality longitudinally may find more robust links between sleep processing and related gains in motor performance. It is also possible that, with more effective task performance and associated awake neural dynamics[78,79,81], efficacy of sleep may change. Precise disruption of sleep processing, specifically SO-spindle coupling in healthy animals, was sufficient to prevent offline performance gains, even when awake task learning was robust[6]. This work also showed that precise modulation of the extent of sleep spindle-SO coupling in healthy animals could either enhance or impede sleep processing. While extension of this work in stroke animals has shown SO-spindle nesting resurges with recovery[14], future animal studies that modulate sleep microarchitecture can study if artificial manipulation of SO-nested spindles or δ wave-nested spindles after stroke are sufficient to enhance or impair motor recovery.

One more limitation of this study is the limited sample size with varying lesion location and size. While we focused on getting patients with cortical lesions, sleep may have been impacted differently for one patient with a primarily subcortical stroke. For example, a stroke in the white matter that impacts thalamocortical networks may impact spindles, believed to have a thalamocortical origin. Future work with a larger sample size with varying stroke-types and incorporation of motor task rehabilitation training and drug manipulation, may provide stronger links to inform drug manipulation during sleep to benefit motor recovery post-stroke.

Author Contributions

B.K.S., R.R., C.M.R. and T.G. contributed to the design of the study. R.R., B.K.S. and A.A. contributed to the analysis of the data. B.K.S., J.M.C. and C.M.R., contributed to the acquisition of data. B.K.S., R.R., C.M.R. and T.G. contributed to the interpretation of the data. B.K.S., R.R., C.M.R. and T.G. contributed to the draft of the article.

Acknowledgment

We would like to thank the patients that participated in this study. We would like to thank the Cedars-Sinai Neurophysiology team that helped in EEG data acquisition and consent especially Cody Holland, Erica Quan and Ho Duong. The study was supported by American Heart Association (AHA; predoctoral fellowship 23PRE1018175 to R.R., postdoctoral fellowship 897265 to A.A. and career development award 847486 to T.G.), National Institutes of Health (NIH)'s National Institute for Neurological Disorders and Stroke (NINDS) (R00NS097620 and R01NS128469 to T.G.), National Science Foundation (award 2048231 to T.G.) and Cedars-Sinai Medical Center. A.A. also received support through Cedars-Sinai's Center for Neural Science and Medicine postdoctoral fellowship.

Conflict of Interest

The authors report no conflicts of interest relevant to this study.

Data Availability Statement

The data that support the findings of this study are available from the corresponding author upon reasonable request.

References

1. Ganguly K, Poo MM. Activity-dependent neural plasticity from bench to bedside. Neuron 2013;80(3):729–41.

2. Ganguly K, Khanna P, Morecraft RJ, Lin DJ. Modulation of neural co-firing to enhance network transmission and improve motor function after stroke. Neuron 2022;110(15):2363–2385.

3. Norrving B, Kissela B. The global burden of stroke and need for a continuum of care. Neurology 2013;80:S5-12.

4. Gulati T, Guo L, Ramanathan DS, et al. Neural reactivations during sleep determine network credit assignment. Nature Neuroscience 2017;20:1277–1284.

5. Ramanathan DS, Gulati T, Ganguly K. Sleep-Dependent Reactivation of Ensembles in Motor Cortex Promotes Skill Consolidation. PLoS Biol 2015;13:e1002263.

6. Kim J, Gulati T, Ganguly K. Competing Roles of Slow Oscillations and Delta Waves in Memory Consolidation versus Forgetting. Cell 2019;179(2):514-526 e13.

7. Gulati T, Ramanathan DS, Wong CC, Ganguly K. Reactivation of emergent task-related ensembles during slow-wave sleep after neuroprosthetic learning. Nat Neurosci 2014;17(8):1107–13.

8. Genzel L, Kroes MC, Dresler M, Battaglia FP. Light sleep versus slow wave sleep in memory consolidation: a question of global versus local processes? Trends Neurosci 2014;37:10–19.

9. Stickgold R. Sleep-dependent memory consolidation. Nature 2005;437:1272–1278.

10. Tononi G, Cirelli C. Sleep and the price of plasticity: from synaptic and cellular homeostasis to memory consolidation and integration. Neuron 2014;81:12–34.

11. de Vivo L, Bellesi M, Marshall W, et al. Ultrastructural evidence for synaptic scaling across the wake/sleep cycle. Science 2017;355:507–510.

12. Klinzing JG, Niethard N, Born J. Mechanisms of systems memory consolidation during sleep. Nat Neurosci 2019;22(10):1598–1610.

13. Ebajemito JK, Furlan L, Nissen C, Sterr A. Application of Transcranial Direct Current Stimulation in Neurorehabilitation: The Modulatory Effect of Sleep. Frontiers in neurology 2016;7:54.

14. Kim J, Guo L, Hishinuma A, et al. Recovery of consolidation after sleep following stroke—interaction of slow waves, spindles, and GABA. Cell Reports 2022;38(9):110426.

15. Backhaus W, Braass H, Gerloff C, Hummel FC. Can Daytime Napping Assist the Process of Skills Acquisition After Stroke? Front Neurol 2018;9:1002.

16. Baumann CR, Kilic E, Petit B, et al. Sleep EEG Changes After Middle Cerebral Artery Infarcts in Mice: Different Effects of Striatal and Cortical Lesions. Sleep 2006;29(10):1339–1344.

17. Duss SB, Seiler A, Schmidt MH, et al. The role of sleep in recovery following ischemic stroke: A review of human and animal data. Neurobiology of Sleep and Circadian Rhythms 2017;2:94–105.

18. Facchin L, Schöne C, Mensen A, et al. Slow Waves Promote Sleep-Dependent Plasticity and Functional Recovery after Stroke. J. Neurosci. 2020;40(45):8637–8651.

19. Gao B, Cam E, Jaeger H, et al. Sleep Disruption Aggravates Focal Cerebral Ischemia in the Rat. Sleep 2010;33(7):879–887.

20. Giubilei F, Iannilli M, Vitale A, et al. Sleep patterns in acute ischemic stroke. Acta Neurologica Scandinavica 1992;86(6):567–571.

21. Gottselig JM, Bassetti CL, Achermann P. Power and coherence of sleep spindle frequency activity following hemispheric stroke. Brain 2002;125(2):373–383.

22. Poryazova R, Huber R, Khatami R, et al. Topographic sleep EEG changes in the acute and chronic stage of hemispheric stroke. Journal of Sleep Research 2015;24(1):54–65.

23. Siengsukon CF, Boyd LA. Sleep to learn after stroke: Implicit and explicit off-line motor learning. Neuroscience Letters 2009;451(1):1–5.

24. Lemke SM, Ramanathan DS, Darevksy D, et al. Coupling between motor cortex and striatum increases during sleep over long-term skill learning. eLife 2021;10:e64303.

25. Born J, Rasch B, Gais S. Sleep to Remember. Neuroscientist 2006;12(5):410–424.

26. Rothschild G, Eban E, Frank LM. A cortical–hippocampal–cortical loop of information processing during memory consolidation. Nat Neurosci 2017;20(2):251–259.

27. Sirota A, Csicsvari J, Buhl D, Buzsáki G. Communication between neocortex and hippocampus during sleep in rodents. Proceedings of the National Academy of Sciences 2003;100(4):2065–2069.

28. Peyrache A, Khamassi M, Benchenane K, et al. Replay of rule-learning related neural patterns in the prefrontal cortex during sleep. Nat Neurosci 2009;12:919–926.

29. Walker MP, Brakefield T, Morgan A, et al. Practice with sleep makes perfect: sleep-dependent motor skill learning. Neuron 2002;35:205–211.

30. Korman M, Doyon J, Doljansky J, et al. Daytime sleep condenses the time course of motor memory consolidation. Nat Neurosci 2007;10:1206–1213.

31. Buzsáki G. Hippocampal sharp wave-ripple: A cognitive biomarker for episodic memory and planning. Hippocampus 2015;25(10):1073–1188.

32. Cairney SA, Guttesen A á V, El Marj N, Staresina BP. Memory Consolidation Is Linked to Spindle-Mediated Information Processing during Sleep. Current Biology 2018;28(6):948-954.e4.

33. Helfrich RF, Mander BA, Jagust WJ, et al. Old Brains Come Uncoupled in Sleep: Slow Wave-Spindle Synchrony, Brain Atrophy, and Forgetting. Neuron 2018;97(1):221-230.e4.

34. Latchoumane C-FV, Ngo H-VV, Born J, Shin H-S. Thalamic Spindles Promote Memory Formation during Sleep through Triple Phase-Locking of Cortical, Thalamic, and Hippocampal Rhythms. Neuron 2017;95(2):424-435.e6.

35. Maingret N, Girardeau G, Todorova R, et al. Hippocampo-cortical coupling mediates memory consolidation during sleep. Nat Neurosci 2016;19(7):959–964.

36. Tu-Chan AP, Natraj N, Godlove J, et al. Effects of somatosensory electrical stimulation on motor function and cortical oscillations. J NeuroEngineering Rehabil 2017;14(1):113.

37. van Dellen E, Hillebrand A, Douw L, et al. Local polymorphic delta activity in cortical lesions causes global decreases in functional connectivity. NeuroImage 2013;83:524–532.

38. Sarasso S, D'Ambrosio S, Fecchio M, et al. Local sleep-like cortical reactivity in the awake brain after focal injury. Brain 2020;143(12):3672–3684.

39. Carmichael ST, Chesselet MF. Synchronous neuronal activity is a signal for axonal sprouting after cortical lesions in the adult. J Neurosci 2002;22:6062–6070.

40. Gulati T, Won SJ, Ramanathan DS, et al. Robust neuroprosthetic control from the stroke perilesional cortex. The Journal of Neuroscience 2015;35:8653–61.

41. Burns BD, Webb AC. The correlation between discharge times of neighbouring neurons in isolated cerebral cortex. Proceedings of the Royal Society of London. Series B. Biological Sciences 1997;203(1153):347–360.

42. Nita DA, Cissé Y, Timofeev I, Steriade M. Waking–Sleep Modulation of Paroxysmal Activities Induced by Partial Cortical Deafferentation. Cerebral Cortex 2007;17(2):272–283.

43. von Elm E, Altman DG, Egger M, et al. The Strengthening the Reporting of Observational Studies in Epidemiology (STROBE) Statement: guidelines for reporting observational studies. Int J Surg 2014;12(12):1495–1499.

44. Martínez-Cagigal V. Topographic EEG/MEG plot [Internet]. 2023;Available from: https://www.mathworks.com/matlabcentral/fileexchange/72729-topographic-eeg-meg-plot

45. Aarts E, Verhage M, Veenvliet JV, et al. A solution to dependency: using multilevel analysis to accommodate nested data. Nat Neurosci 2014;17(4):491–6.

46. Cassidy JM, Wodeyar A, Wu J, et al. Low-Frequency Oscillations Are a Biomarker of Injury and Recovery After Stroke. Stroke 2020;51(5):1442–1450.

47. Topolnik L, Steriade M, Timofeev I. Partial Cortical Deafferentation Promotes Development of Paroxysmal Activity. Cerebral Cortex 2003;13(8):883–893.

48. Antony JW, Piloto L, Wang M, et al. Sleep Spindle Refractoriness Segregates Periods of Memory Reactivation. Current Biology 2018;28(11):1736-1743.e4.

49. Staresina BP, Bergmann TO, Bonnefond M, et al. Hierarchical nesting of slow oscillations, spindles and ripples in the human hippocampus during sleep. Nat Neurosci 2015;18(11):1679–1686.

50. Bergmann TO, Born J. Phase-Amplitude Coupling: A General Mechanism for Memory Processing and Synaptic Plasticity? Neuron 2018;97(1):10–13.

51. Bhattacharya S, Donoghue JA, Mahnke M, et al. Propofol Anesthesia Alters Cortical Traveling Waves. Journal of Cognitive Neuroscience 2022;34(7):1274–1286.

52. Soplata AE, Adam E, Brown EN, et al. Rapid thalamocortical network switching mediated by cortical synchronization underlies propofol-induced EEG signatures: a biophysical model [Internet]. 2023;2022.02.17.480766.[cited 2023 Apr 10] Available from: https://www.biorxiv.org/content/10.1101/2022.02.17.480766v2

53. Purcell SM, Manoach DS, Demanuele C, et al. Characterizing sleep spindles in 11,630 individuals from the National Sleep Research Resource. Nat Commun 2017;8(1):15930.

54. Andrillon T, Nir Y, Staba RJ, et al. Sleep Spindles in Humans: Insights from Intracranial EEG and Unit Recordings. J. Neurosci. 2011;31(49):17821–17834.

55. Riedner BA, Vyazovskiy VV, Huber R, et al. Sleep Homeostasis and Cortical Synchronization: III. A High-Density EEG Study of Sleep Slow Waves in Humans. Sleep 2007;30(12):1643–1657.

56. Bauerschmidt A, Al-Bermani T, Ali S, et al. Modern Sedation and Analgesia Strategies in Neurocritical Care. Curr Neurol Neurosci Rep 2023;

57. Kang Y, Saito M, Toyoda H. Molecular and Regulatory Mechanisms of Desensitization and Resensitization of GABAA Receptors with a Special Reference to Propofol/Barbiturate. Int J Mol Sci 2020;21(2):563.

58. Ouyang W, Wang G, Hemmings HC. Isoflurane and propofol inhibit voltage-gated sodium channels in isolated rat neurohypophysial nerve terminals. Mol Pharmacol 2003;64(2):373–381.

59. Tang P, Eckenhoff R. Recent progress on the molecular pharmacology of propofol. F1000Res 2018;7:123.

60. Lynch BA, Lambeng N, Nocka K, et al. The synaptic vesicle protein SV2A is the binding site for the antiepileptic drug levetiracetam. Proc Natl Acad Sci U S A 2004;101(26):9861–9866.

61. Luz Adriana PM, Blanca Alcira RM, Itzel Jatziri CG, et al. Effect of levetiracetam on extracellular amino acid levels in the dorsal hippocampus of rats with temporal lobe epilepsy. Epilepsy Research 2018;140:111–119.

62. Bell C, Vanderlinden H, Hiersemenzel R, et al. The effects of levetiracetam on objective and subjective sleep parameters in healthy volunteers and patients with partial epilepsy. Journal of Sleep Research 2002;11(3):255–263.

63. Bazil CW, Battista J, Basner RC. Effects of levetiracetam on sleep in normal volunteers. Epilepsy & Behavior 2005;7(3):539–542.

64. Murphy M, Bruno M-A, Riedner BA, et al. Propofol Anesthesia and Sleep: A High-Density EEG Study. Sleep 2011;34(3):283–291.

65. Yeh W-C, Lu S-R, Wu M-N, et al. The impact of antiseizure medications on polysomnographic parameters: a systematic review and meta-analysis. Sleep Medicine 2021;81:319–326.

66. Purdon PL, Pierce ET, Mukamel EA, et al. Electroencephalogram signatures of loss and recovery of consciousness from propofol. Proc Natl Acad Sci U S A 2013;110(12):E1142-1151.

67. Bernhardt J, Hayward KS, Kwakkel G, et al. Agreed Definitions and a Shared Vision for New Standards in Stroke Recovery Research: The Stroke Recovery and Rehabilitation Roundtable Taskforce. Neurorehabil Neural Repair 2017;31(9):793–799.

68. Pearson-Fuhrhop KM, Kleim JA, Cramer SC. Brain Plasticity and Genetic Factors. Topics in Stroke Rehabilitation 2009;16(4):282–299.

69. Ganguly K, Byl NN, Abrams GM. Neurorehabilitation: Motor recovery after stroke as an example. Annals of Neurology 2013;74(3):373–381.

70. Dromerick AW, Lang CE, Birkenmeier RL, et al. Very Early Constraint-Induced Movement during Stroke Rehabilitation (VECTORS): A single-center RCT. Neurology 2009;73(3):195–201.

71. Dromerick AW, Geed S, Barth J, et al. Critical Period After Stroke Study (CPASS): A phase II clinical trial testing an optimal time for motor recovery after stroke in humans. Proceedings of the National Academy of Sciences 2021;118(39):e2026676118.

72. Krakauer JW, Carmichael ST, Corbett D, Wittenberg GF. Getting Neurorehabilitation Right: What Can Be Learned From Animal Models? Neurorehabil Neural Repair 2012;26(8):923–931.

73. Clarkson AN, Huang BS, MacIsaac SE, et al. Reducing excessive GABA-mediated tonic inhibition promotes functional recovery after stroke. Nature 2010;468(7321):305–309.

74. He W-M, Ying-Fu L, Wang H, Peng Y-P. Delayed treatment of α5 GABAA receptor inverse agonist improves functional recovery by enhancing neurogenesis after cerebral ischemia-reperfusion injury in rat MCAO model. Sci Rep 2019;9(1):2287.

75. Marshall L, Helgadottir H, Molle M, Born J. Boosting slow oscillations during sleep potentiates memory. Nature 2006;444:610–613.

76. Ngo H-VV, Martinetz T, Born J, Mölle M. Auditory Closed-Loop Stimulation of the Sleep Slow Oscillation Enhances Memory. Neuron 2013;78(3):545–553.

77. Levy RM, Harvey RL, Kissela BM, et al. Epidural Electrical Stimulation for Stroke Rehabilitation: Results of the Prospective, Multicenter, Randomized, Single-Blinded Everest Trial. Neurorehabil Neural Repair 2016;30(2):107–119.

78. Khanna P, Totten D, Novik L, et al. Low-frequency stimulation enhances ensemble co-firing and dexterity after stroke [Internet]. Cell 2021;Available from: https://www.ncbi.nlm.nih.gov/pubmed/33571430

79. Ramanathan DS, Guo L, Gulati T, et al. Low-frequency cortical activity is a neuromodulatory target that tracks recovery after stroke. Nat Med 2018;24(8):1257–1267.

80. Abbasi A, Danielsen NP, Leung J, et al. Epidural cerebellar stimulation drives widespread neural synchrony in the intact and stroke perilesional cortex. Journal of NeuroEngineering and Rehabilitation 2021;18(1):89.

81. Guo L, Kondapavulur S, Lemke SM, et al. Coordinated increase of reliable cortical and striatal ensemble activations during recovery after stroke. Cell Reports 2021;36(2):109370.

Figure captions

Figure 1. Stroke versus contralateral electrode assignment. 10-20 system for EEG showing locations of all electrode locations recorded with an illustration of stroke. Grey shaded area shows a representative stroke perilesional region. Blue shaded circles represent mastoid electrodes (A1, A2) that were used for referencing. Red circles indicate identified *Stroke electrodes* based on proximity to the perilesional area. Green circles indicate identified *Contralateral electrodes* which are mirror/contralateral to identified *Stroke electrodes.* T5/P7 and T6/P8 are used interchangeably for this analysis.

Figure 2. NREM sleep oscillations. A, Representative 20 identified *δ* wave waveforms (gray traces) with their mean shown in black for an example EEG channel in one patient; **B,** Mean *δ* wave along with s.e.m. (standard error of mean) bands (blue) for all identified *δ* waves from an example channel from EEG data recording for one patient. **C, D,** Same as A, B for SOs. **E, F,** Same as A, B for spindle waveforms. All waveforms are centered around the detected states. **G,** Cartoon of SO-spindle nesting. Nesting window was –0.5 to +1.0 s from SO up state as shown. **H,** Cartoon of *δ* wave-spindle nesting. Nesting window –0.5 to +1.0 s from δ up state as depicted.

Figure 3. Patient imaging data and topographical density plots for different NREM oscillations. Top to bottom: ***Imaging data***: CT (computed tomography) image for patient P1, T2 sequences of MRI (magnetic resonance imaging) images for patients P2 to P5. Radiologic imaging has been flipped horizontally to align with topographic density maps; *i.e.*, image left, and right are ipsilateral to patient left and right. Left and right are marked in imaging figures (P1-P5) and apply to density topographical maps below them; ***Topographical map*** for detected ***spindle*** density (count/min) during NREM sleep for all patients; ***Topographical map*** for detected ***SO*** density (count/min) during NREM sleep for all patients; ***Topographical map*** for detected ***δ waves'*** density (count/min) during NREM sleep for all patient; ***Topographical map*** for detected ***nested SO-spindle*** density (count/min) during NREM sleep for all patients; ***Topographical map*** for detected ***δ waves-nested-spindle*** density (count/min) during NREM sleep for all patients.

Figure 4. NREM oscillations' density for different patient groups on stroke verses contralateral electrodes. A, Table showing selected *stroke* and *contralateral electrodes* for all patients. **B,** Comparison of *δ wave* density (count/min) on *stroke versus contralateral electrode*s for patients on different medications[#]. Black line shows the mean values within the group. **C,** Same as B for SO density. **D,** Same as B for spindle density. **E,** Same as B for nested *δ* wave-nested spindle density. **F,** Same as B for SO-nested spindle density. [#]Patient medication groups: *(i)* Group 1: propofol (P1); *(ii)* Group 2: levetiracetam (brand name: Keppra) (P2 & P5); and *(iii)* Group 3: non-neuromodulatory drugs (P3 & P4). *: statistically significant *p* values for two-tailed *t*-test.

Table

Patient	P1	P2	P3	P4	P5
Stroke location	R MCA	R MCA	L MCA	R MCA	R MCA
Time of recording after stroke	2 days	2 days	3 days	3 days	3 days
Comorbidities	COVID	Partial status (right temporal)	ESRD, HFrEF	Pituitary macroadenoma, Central hypoT	Ruptured R MCA aneurysm
Rx (concurrent)	Propofol gtt Dexamethasone Remdesivir	Levetiracetam Acyclovir Vancomycin Cefepime	ASA/Plavix	ASA Levothyroxine	Levetiracetam Levophed

Table 1. Patient clinical information. Top to bottom, information for five patients P1 to P5. Stroke location; days from stroke when the EEG data was acquired; associated co-morbidities; concurrent medications during EEG recording. R/ L MCA: Right/ left middle cerebral artery; COVID: Coronavirus disease - 2019; ESRD: End-stage renal disease; HFrEF: Heart failure with reduced ejection fraction; HypoT: hypothyroidism; ASA: Acetylsalicylic Acid (Aspirin).

Figure 1

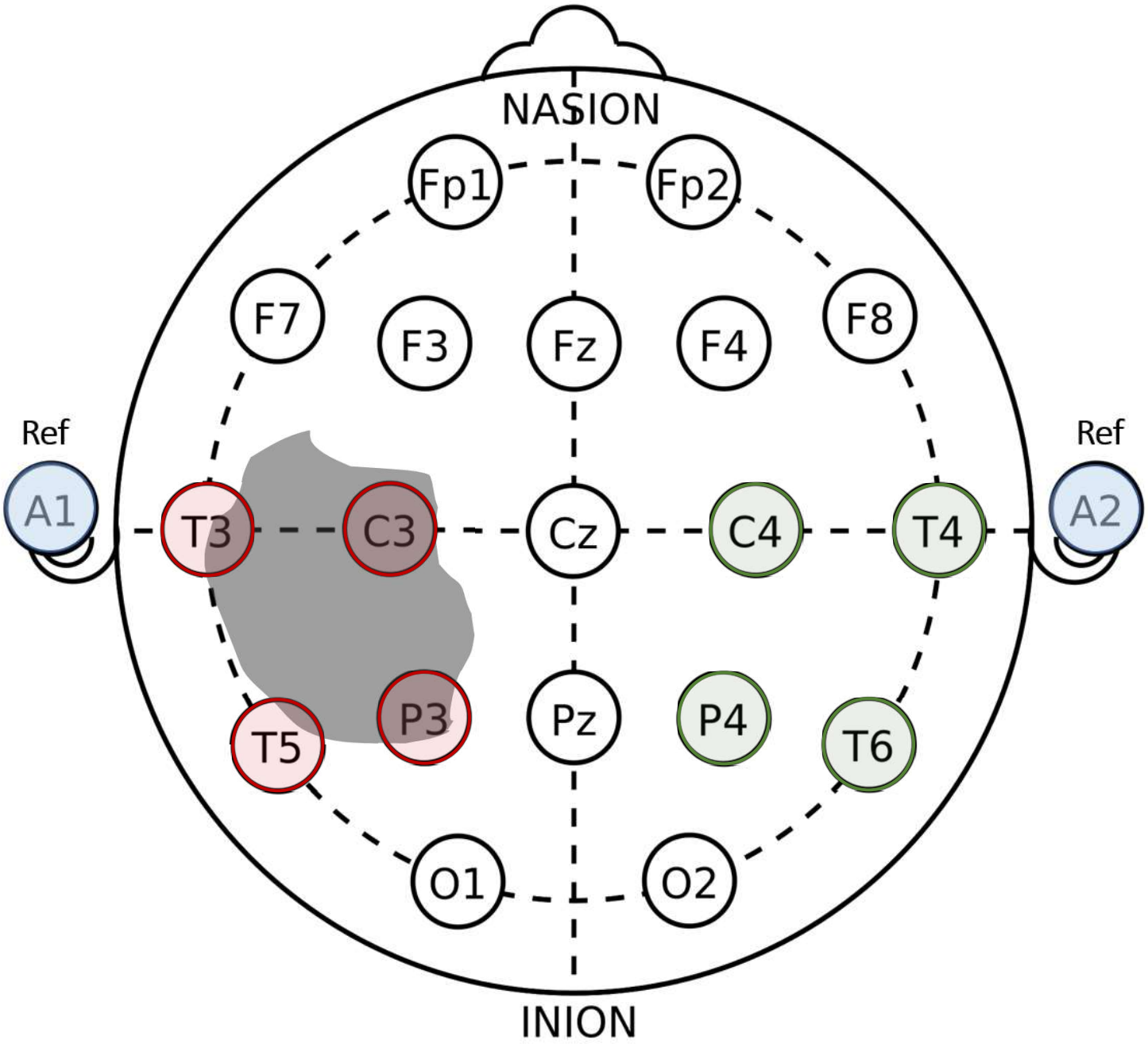

Figure 1. Stroke versus contralateral electrode assignment. 10-20 system for EEG showing locations of all electrode locations recorded with an illustration of stroke. Grey shaded area shows a representative stroke perilesional region. Blue shaded circles represent mastoid electrodes (A1, A2) that were used for referencing. Red circles indicate identified *Stroke electrodes* based on proximity to the perilesional area. Green circles indicate identified *Contralateral electrodes* which are mirror/contralateral to identified *Stroke electrodes.* T5/P7 and T6/P8 are used interchangeably for this analysis.

Figure 2

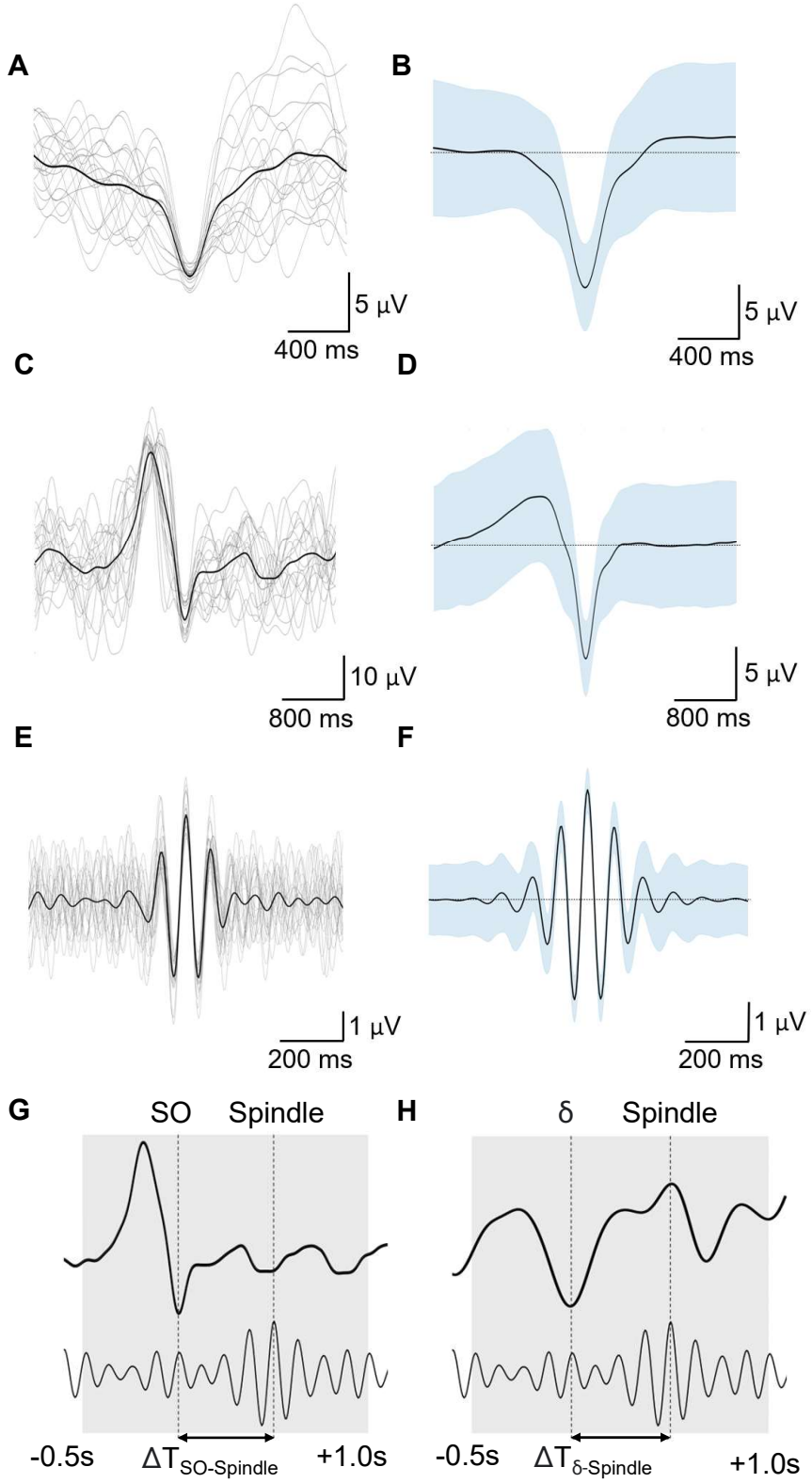

Figure 2. NREM sleep oscillations. A, Representative 20 identified *δ* wave waveforms (gray traces) with their mean shown in black for an example EEG channel in one patient; **B,** Mean *δ* wave along with s.e.m. (standard error of mean) bands (blue) for all identified *δ* waves from an example channel from EEG data recording for one patient. **C, D,** Same as A, B for SOs. **E, F,** Same as A, B for spindle waveforms. All waveforms are centered around the detected states. **G,** Cartoon of SO-spindle nesting. Nesting window was –0.5 to +1.0 s from SO up state as shown. **H,** Cartoon of *δ* wave-spindle nesting. Nesting window –0.5 to +1.0 s from δ up state as depicted.

Figure 3

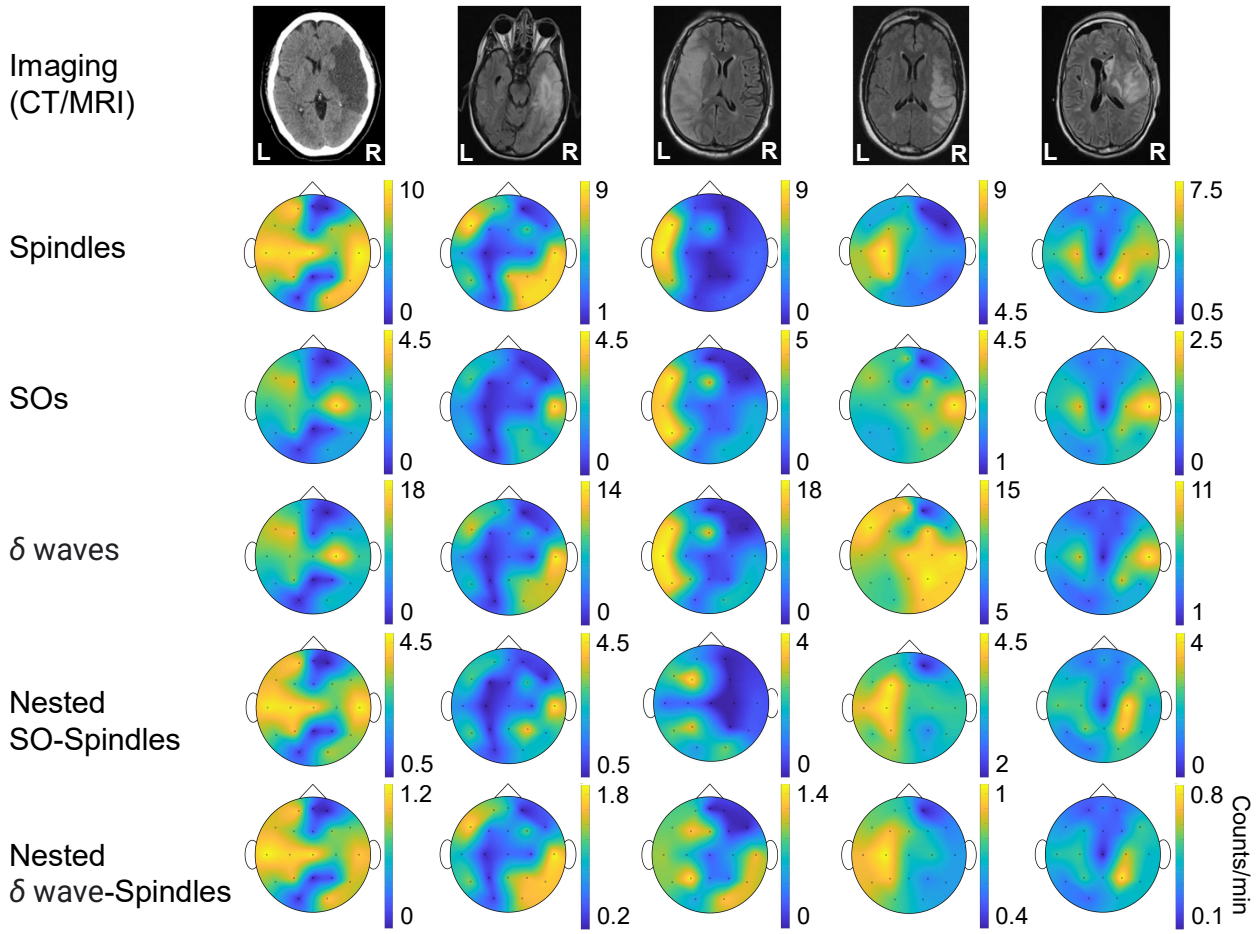

Figure 3. Patient imaging data and topographical density plots for different NREM oscillations. Top to bottom: ***Imaging data***: CT (computed tomography) image for patient P1, T2 sequences of MRI (magnetic resonance imaging) images for patients P2 to P5. Radiologic imaging has been flipped horizontally to align with topographic density maps; *i.e.*, image left, and right are ipsilateral to patient left and right. Left and right are marked in imaging figures (P1-P5) and apply to density topographical maps below them; ***Topographical map*** for detected ***spindle*** density (count/min) during NREM sleep for all patients; ***Topographical map*** for detected ***SO*** density (count/min) during NREM sleep for all patients; ***Topographical map*** for detected ***δ waves'*** density (count/min) during NREM sleep for all patient; ***Topographical map*** for detected ***nested SO-spindle*** density (count/min) during NREM sleep for all patients; ***Topographical map*** for detected ***δ waves-nested-spindle*** density (count/min) during NREM sleep for all patients.

Figure 4

A

Patient	P1	P2	P3	P4	P5
Stroke electrodes	C4,F8, T4,T6/ P8	T4,P4, T6/P8	C3,F7, P3,T3, O1,T5 /P7,F3	P4,F8, T4,T6/ P8	C4,F8, T4,T6/ P8
Contralateral electrodes	C3,F7, T3,T5/ P7	T3,P3, T5/P7	C4,F8, P4,T4, O2,T6 /P8,F3	P3,F7, T3,T5/ P7	C3,F7, T3,T5/ P7

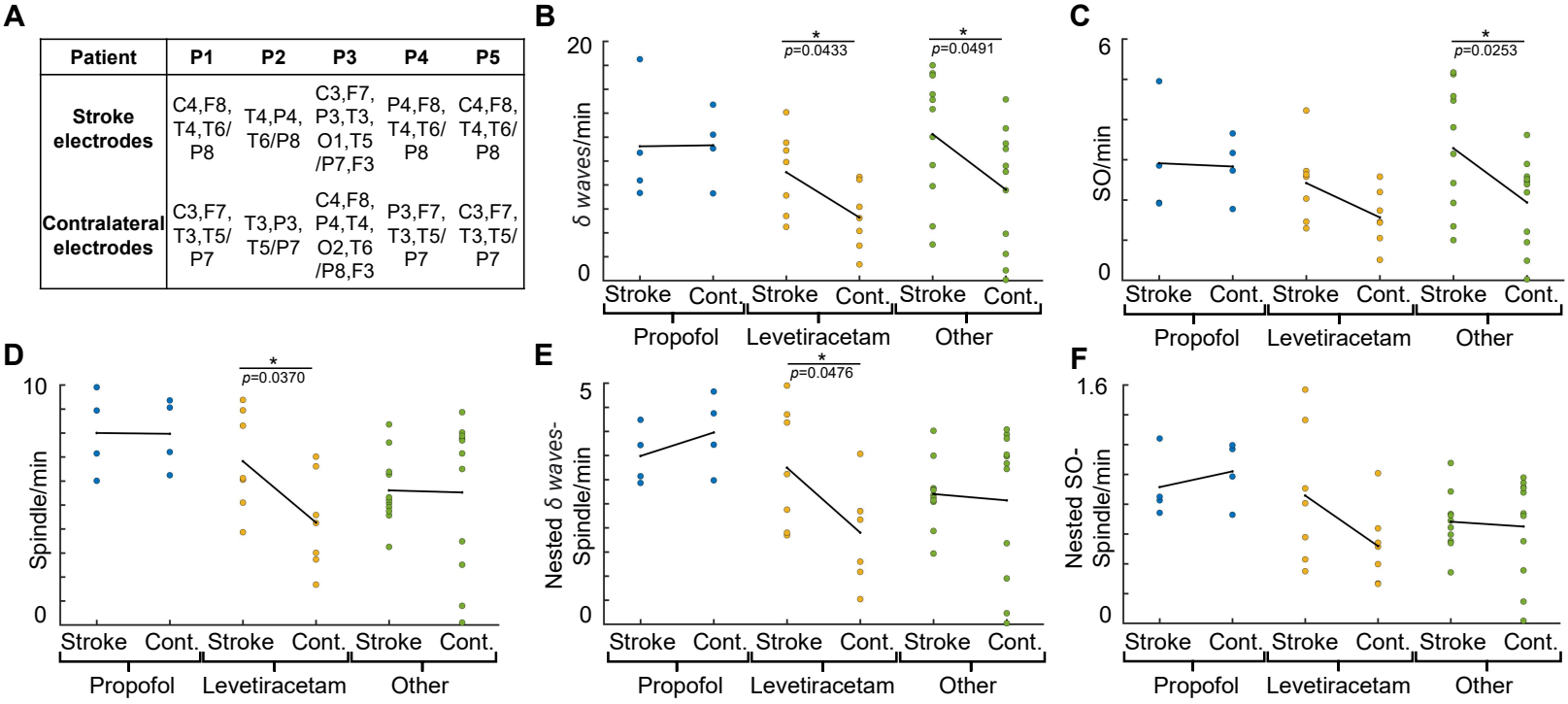

Figure 4. NREM oscillations' density for different patient groups on stroke verses contralateral electrodes. **A,** Table showing selected *stroke* and *contralateral electrodes* for all patients. **B,** Comparison of *δ wave* density (count/min) on *stroke versus contralateral electrode*s for patients on different medications#. Black line shows the mean values within the group. **C,** Same as B for SO density. **D,** Same as B for spindle density. **E,** Same as B for nested *δ* wave-nested spindle density. **F,** Same as B for SO-nested spindle density. #Patient medication groups: *(i)* Group 1: propofol (P1); *(ii)* Group 2: levetiracetam (brand name: keppra) (P2 & P5); and *(iii)* Group 3: non-neuromodulatory drugs (P3 & P4). *: statistically significant *p* values for two-tailed *t*-test.